

1 Title: Stochastic model for the fluctuations of the atmospheric concentration of radionuclides and its
2 application to uncertainty evaluation

3 Hiroyuki Ichige, Shun Fukuchi, Yuko Hatano
4 Graduate School of Systems and Information Engineering, University of Tsukuba

Keywords: Chernobyl, risk assessment, stochastic process, time-series analysis, radionuclide

Telephone number: +8190-1032-7643

Email: tanuki28213141@gmail.com

5 Abstract:

6 We propose a new model of the atmospheric concentration of a radionuclide with the inclusion of
7 fluctuations of the concentration. The model is a stochastic differential equation and we derive the
8 analytic solution of the equation. The solution agrees very well with the Chernobyl Cs-137 data.
9 The advantage of the model is that the uncertainty in radiation exposure risk, with regard to the
10 concentration fluctuations, can be quantitatively estimated. We show the range of fluctuations of $\pm\sigma$,
11 $\pm 2\sigma$, $\pm 3\sigma$ in the 10-year measurement of the atmospheric concentration in Chernobyl and confirmed
12 the validity of the model.

13 1. Introduction

14 In major nuclear power plant accidents, such as Chernobyl or Fukushima, a huge amount of
15 radionuclides have been released into the atmosphere. In such accidents, long-lived radionuclides,
16 cesium-137 and strontium-90, for example, pose a serious problem. Radionuclides carried in the
17 initial plume were deposited on the ground, and they keep imposing a risk to the public health for a
18 long period of time. In the Chernobyl case, it is believed that the resuspension-deposition cycle
19 contributes significantly to the airborne concentration of radionuclides (Klug et al., 1992; Ishikawa,
20 1995; Nicholson, 1998; Ould-Dada and Nasser, 1992). Since the resuspended nuclides make the
21 atmospheric concentration increase, it is considered one of the most important processes in the
22 long-term radiation risk assessment. In this accident, health effects on the humans, such as leukemia
23 and genetic abnormalities have been confirmed (IAEA, 2006; Arkhipov et al., 1994; Lazjukd et al.,

24 1997; Romanenko et al., 2008). Therefore precise predictions on the concentrations of radionuclides
25 are necessary.

26 For that purpose, using the data of the Chernobyl accident, we have derived a simple formula on
27 the mean atmospheric concentration (Hatano et al., 1997, 1998). In the formula, the atmospheric
28 concentration of a specific radionuclide decreases as

$$C(t) = A \exp(-\lambda_{phys} t) t^{-\alpha}. \quad (1)$$

29 Here $C(t)$ is the concentration of a specific radionuclide measured at a fixed location, t is the
30 number of days since the accident, λ_{phys} is the rate constant which includes all the first-order
31 reactions (*e.g.* radioactive decay, adsorption rate on the soil, see Hatano and Hatano, 1997). A and
32 α are constants that is determined by the fitting of the actual data. The power index $-\alpha$ in Eq. (1)
33 is determined from the magnitude of the temporal autocorrelations of the wind velocity. In our
34 previous studies (Hatano et al., 1997, 1998), we set α at $-\frac{4}{3}$. Equation (1) successfully reproduces
35 the mean concentration of the Chernobyl data (Cs-137-134, Ce-144, Ru-106) over a decade. In
36 present study, we allow more degrees of freedom on α , because the wind correlation may vary
37 depending on sites. In this manner, we introduce more flexibility to the model and thereby make the
38 model applicable in general cases. For the details of our model, see the references. We would stress
39 that Eq. (1) is derived by averaging out all the fluctuations of microscopic processes; therefore it
40 describes the mean behavior of the atmospheric concentration.

41 In the present study, we concentrate on how the data fluctuates from Eq. (1), and thereby estimate
42 the maximum and the minimum concentrations of the atmospheric concentration. From the
43 Chernobyl case, we have learned that the atmospheric concentration of radionuclides fluctuates very
44 much, depending mainly on the meteorological conditions (the wind velocity, the humidity, rainfall,
45 the amount of solar radiation, and the traffics). Estimating the magnitude of fluctuations would
46 greatly contributes for radiation safety. For this purpose we proposed a model that can reproduce
47 those fluctuations.

48 2. Model --- stochastic differential equation on the fluctuations

49 In this section, we propose a new model that can reproduce the fluctuations in the Cs-137
50 atmospheric concentration. The model is a stochastic differential equation, assuming that each
51 deviation follows a stochastic process. We use here the Chernobyl data set. The measurement site is
52 shown in Fig. 1 based on the report of the Japan Atomic Energy Research Institute (Ueno et al.,

53 2003). We choose 6 observation sites. Each site is assigned a number, e.g. "Point 20.0". The sites
 54 we choose are Point 6.0 (7 km to the southwest from the power plant), Point 8.0 (11 km, north),
 55 Point 11.0 (10 km, south), Point 13.0 (9 km, east), Point 21.0 (2 km, northwest), and Point 60.1 (3
 56 km, northwest). These sites have longer observation period than others. As the radionuclide, we
 57 choose Cs-137, because Cs-137 was detectable over a decade because of their long half-life
 58 (~30years) and amount released was also very large. In Fig. 2, we show a good agreement between
 59 Eq. (1) and the data at Point 21.0 for a demonstrating purpose. Other graphs appear in Hatano et al.,
 60 1998.

61 Figure 3 shows the raw data of the atmospheric concentration of Cs-137 at Point 13.0 for 5000
 62 days after the accident. The airborne concentration of Cs-137 fluctuates by various reasons: for
 63 example, wind transport from other places, ground surface disturbances such as rainfall, and
 64 detachment from surfaces such as trees or buildings. We assume that if we take a long enough
 65 period of time, these elementary processes achieve the equilibrium of fluctuations and can be
 66 treated as a stationary stochastic process. The repeated randomness is manifest as the resulting
 67 averaged behavior. We assume here that these fluctuations of the elementary processes are the
 68 Gaussian white noise. The Gaussian white noise is observed frequently in natural phenomena.

69 We model those fluctuations by means of the stochastic differential equation as follows. First, we
 70 define the residual, $X(t)$, between the data and Eq. (1), as

$$\begin{aligned} X(t) &= \ln\left(C(t)/(A\exp(-\lambda_{phys}t)t^{-\alpha})\right) \\ &= \ln(C(t)) - \ln(A\exp(-\lambda_{phys}t)t^{-\alpha}). \end{aligned} \quad (2)$$

71 In Fig. 4 we see the behavior of $X(t)$ for Point 13.0. When we see $X(t)$ as a stochastic variable,
 72 we observe the following two things. One is that the negative values of $X(t)$ and the positive
 73 values of that appear almost at the same frequency throughout the measurement. Second, the
 74 displacement in $X(t)$ is almost *reversal*. Namely, if $X(t_i) > X(t_{i-1})$, then it is likely we have
 75 $X(t_{i+1}) < X(t_i)$ in the next time step, and *vice versa*. Therefore, the model may have the property
 76 of a correction force that neutralizes fluctuations:

$$E\left[\frac{dX(t)}{dt}\right] = -\gamma X, \quad (3)$$

77 or

$$E[dX(t)] = -\gamma X dt. \quad (4)$$

78 Here $E[\]$ represents the expected value and $dX(t)$ is the displacement in X during small amount
 79 of time dt . We assume that the sum of $dX(t)$ and $\gamma X dt$ is the Gaussian white noise. That is,

$$dX(t) = -\gamma X dt + \sigma dW(t). \quad (5)$$

80 Here $dW(t)$ is the Gaussian white noise at time t , and γ is the parameter of the "reversal" force,

81 and σ is the parameter indicating the magnitude of the Gaussian white noise. The stochastic
 82 differential equation Eq. (5) is called as the Ornstein-Uhlenbeck process. If the Chernobyl data
 83 fluctuate as Eq. (5), we should recover the Gaussian white noise $\sigma dW(t)$ by substituting the actual
 84 data $dX + \gamma X dt$. In order to show that, we first estimate the values of γ and σ in the next section.

85 3. Results and discussion

86 3.1 Estimation of parameters γ and σ

87 In estimating the values of γ and σ , we demonstrate in Fig. 5 how the value of γ works on
 88 $X(t)$. The horizontal axis is $X(t)$ at Point 21.0 over 5000 days, and the vertical axis is its
 89 derivative $dX(t)/dt$. The straight line is the LSM (Least Squares Method) fit to the data.
 90 According to Eq. (3), the slope in Fig. 5 corresponds to the value $-\gamma$. As shown in this figure, we
 91 see a fairly good fit. The actual data have the tendency that an increase in X at a specific time
 92 results in a decrease in X at the next moment, and vice versa. However, the LSM fit in Fig. 5 is, in
 93 some part, not so good. This is due to the fact that the value of dt (time interval between
 94 observations) is sometimes very large in the actual data. In an extreme case, dt is about 30 days.
 95 Therefore, in the following, we calculate more accurate value of γ .

96 Let us start with Eq. (5). Solution of Eq. (5) is given by Susanne and Ove, 2008.

$$X(t) = \exp(-\gamma t) \left[X(t_0) + \sigma \int_0^t \exp(\gamma s) dW(s) \right], \quad (6)$$

97 where $X(t_0)$ is the initial value. Because $X(t)$ is the discrete in the actual data, we rewrite it as
 98 $X(t_0), X(t_1), X(t_2), \dots, X(t_i), \dots, X(t_n)$. Due to the Markov property of Wiener process, it is
 99 possible to take the initial value at anywhere and Eq. (6) can also be expressed as follows:

$$\begin{aligned} & X(t_{i+1}) - \exp(-\gamma(t_{i+1} - t_i)) X(t_i) \\ &= \sigma \exp(-\gamma(t_{i+1} - t_i)) \int_0^{t_{i+1} - t_i} \exp(\gamma s) dW(s). \end{aligned} \quad (7)$$

100 If you replace t_i to 0 and $t_{i+1} - t_i$ to t , then Eq. (7) and Eq. (6) are equivalent. Hence, we define
 101 the value of the right-hand side of Eq. (7) as Y :

$$Y = \sigma \exp[-\gamma(t_{i+1} - t_i)] \sum_{j=0}^K \exp(\gamma s_j) [W(s_{j+1}) - W(s_j)]. \quad (8)$$

102 Here K is the number of discretization in s . From the definition of the Wiener process,
 103 $W(s_{j+1}) - W(s_j)$ is a random variable and follows the normal distribution with 0-mean and the
 104 variance $s_{j+1} - s_j$. Since the sum of the random variables, which follow the normal distribution,
 105 also follows the normal distribution, Y follows the normal distribution. The mean of the sum is

106 equal to 0, and the variance is follows from simple calculation:

$$V[Y] = \sigma^2 \exp(-2\gamma(t_{i+1} - t_i)) \times E \left[\sum_{j=0}^K \exp(2\gamma t_j) (W(s_{j+1}) - W(s_j))^2 \right]. \quad (9)$$

107 Here $V[\]$ represents the variance and we use the relation $V[Y] = E[Y^2] - (E[Y])^2$ for
 108 calculation. Using $(W(s_{j+1}) - W(s_j))^2 = s_{j+1} - s_j$, we obtained the following equation:

$$V[Y] = \sigma^2 \exp(-2\gamma(t_{i+1} - t_i)) \int_0^{t_{i+1}-t_i} \exp(2\gamma s) ds. \quad (10)$$

109 By solving this, Y , or the entire right side of Eq. (7) is a random variable that follows the normal
 110 distribution with 0-mean and with the variance $\sigma^2(1 - \exp(-2\gamma(t_{i+1} - t_i)))/2\gamma$. Note that
 111 variance solely depends on $(t_{i+1} - t_i)$. It means that, when the interval between observations is
 112 long, the variance of the fluctuations increases. On the contrary, when the interval is small, the
 113 variance of fluctuations decreases. In order to eliminate this dependence on the interval length, we

114 normalize Eq. (7) by dividing the both sides with $1 - \exp(-2\gamma(t_{i+1} - t_i))^{\frac{1}{2}}$ to obtain

$$\begin{aligned} & \frac{X(t_{i+1}) - \exp(-\gamma(t_{i+1} - t_i))X(t_i)}{\sqrt{1 - \exp(-2\gamma(t_{i+1} - t_i))}} \\ &= \frac{\sigma \exp(-\gamma(t_{i+1} - t_i)) \int_0^{t_{i+1}-t_i} \exp(2\gamma t) dW(s)}{\sqrt{1 - \exp(-2\gamma(t_{i+1} - t_i))}}. \end{aligned} \quad (11)$$

115 Now the entire right-hand side of Eq. (11) is a random variable that follows the normal distribution
 116 with 0-mean and the variance $\sigma^2/2\gamma$. In addition, with respect to the left-hand side, all parameters
 117 are known except for γ . Hence, γ is obtained by the following equation.

$$\sum_{i=1}^n \frac{X(t_{i+1}) - \exp(-\gamma(t_{i+1} - t_i))X(t_i)}{\sqrt{1 - \exp(-2\gamma(t_{i+1} - t_i))}} \text{sgn}X(t_i) = 0. \quad (12)$$

118 Here $\text{sgn}(x)$ is the signum function defined as follows.

$$\text{sgn}(x) = \begin{cases} -1 & (x < 0) \\ 0 & (x = 0) \\ 1 & (x > 0) \end{cases} \quad (13)$$

119 Then substituting thus-obtained γ to Eq. (11), we finally arrive at the equation for σ .

$$\sigma^2 = 2\gamma \sum_{i=1}^n \left(\frac{X(t_{i+1}) - \exp(-\gamma(t_{i+1} - t_i))X(t_i)}{\exp(-2\gamma(t_{i+1} - t_i))} \right)^2. \quad (14)$$

120 To summarize, we can calculate the parameters γ and σ with Eq. (12) and Eq. (14), using the
 121 actual data. We summarize the values of γ and σ of each observation site in Table1. These values

122 are used in the calculations in the next subsection.

123 3.2 Analytic Solution

124 In Section 3.1, we explained that, in order to show that $X(t)$ can be described by the Eq. (5),
125 $dX + \gamma X dt$ should be the Gaussian white noise. This is equivalent to that the right side of Eq. (11)
126 is the Gaussian white noise. We use the spectral analysis because the Gaussian white noise has the
127 same power in its all frequencies.

128 The result is shown in Fig. 6. The horizontal axis represents the frequency and the vertical axis
129 represents the intensity of the spectrum. Since observation times are unevenly spaced, we used the
130 periodogram (Scargle, 1982; Schulz and Stattegger, 1997). The periodogram is one of the methods of
131 detecting a periodic signal hidden in the noise in the case where the observation times are unevenly
132 spaced. It is used instead of FFT in such cases. Except for a strong annual peak (and its
133 subharmonics), the spectrum scales roughly as the white noise. Figure 6 is the spectrum of Point
134 21.0 and we confirmed that other five observation sites have the very similar white noise spectrum.
135 In this way, our assumption used in Eq. (5) is justified for the present data set.

136 In Fig. 7, we plot the cumulative histogram of the right-hand side of Eq. (11) and found that it
137 follows the normal distribution excellently. The curve showing along with the histogram represents
138 the distribution function of the normal distribution. The values of the mean and the variance were
139 obtained in Section 3.1. Figure 7 is the case for Point 21.0, and we found that the results of other
140 five observation sites are almost identical with Fig. 7. As a result of these findings, it can be said
141 that Eq. (5) is suitable for modeling the fluctuations.

142 Finally we arrive at the analytic solution of radioactive aerosols in the atmosphere. Using Eqs. (2),
143 (5), and (7):

$$C(t) = A \exp(-\lambda_{phys} t) t^{-\alpha} \times \exp \left\{ \exp[-\gamma(t - t_0)] \left[X(t_0) + \sigma \int_0^{t-t_0} \exp[\gamma(t - t_0)] dW(s) \right] \right\}. \quad (15)$$

144 By taking the logarithm on both sides of Eq. (11), we have

$$\ln C(t) = \ln[A \exp(-\lambda_{phys} t) t^{-\alpha}] + \exp[-\gamma(t - t_0)] \left[X(t_0) + \sigma \int_0^{t-t_0} \exp[\gamma(t - t_0)] dW(s) \right]. \quad (16)$$

145 The right-hand side of Eq. (16) is a random variable that follows the normal distribution with the
146 mean $\hat{\mu}$ and the variance $\hat{\sigma}^2$ where

$$\hat{\mu} = \ln[A \exp(-\lambda_{phys} t) t^{-\alpha}] + X(t_0) \exp[-\gamma(t - t_0)]. \quad (17)$$

$$\hat{\sigma}^2 = \frac{\sigma^2}{2\gamma} (1 - \exp[-2\gamma(t - t_0)]) \quad (18)$$

147 Note that, for large t , $\hat{\mu}$ converges to the logarithm of Eq. (1). Thus we obtain the following
 148 equation describing the distribution of the fluctuation.

$$p(t_0, X(t_0), t, X(t)) = \frac{1}{\sqrt{2\pi\hat{\sigma}^2}} e^{-\frac{(X(t)-\hat{\mu})^2}{2\hat{\sigma}^2}}. \quad (19)$$

149 Here p is the transition probability density function; p is the probability where the residual $X(t)$
 150 occurs when the initial residual is $X(t_0)$. To be precise, p describes the probability density of $X(t)$
 151 under the initial condition:

$$\lim_{t \rightarrow t_0} p = \delta(X(t) - X(t_0)). \quad (20)$$

152 Note that $X(t)$ corresponds to $\ln C(t)$ (see Eq. (2)). The right-hand side of Eq. (19) is in the form of
 153 the normal distribution, $C(t)$ obeys the log-normal distribution.

154 In Fig. 8, we summarize the significance of the present study. Let us consider the circumstance in
 155 which we have to predict the future concentration. In usual case (upper half of Fig. 8), we calculate
 156 the average using the observed data that are available at the moment. The future concentration is
 157 estimated by extrapolation. However, the estimation depends on the extrapolation technique (upper
 158 half right). The ranges of fluctuations are sometimes assumed by the maximum and the minimum
 159 values.

160 In the present study, the fluctuation (the difference from one observation to another) gives
 161 information of the future concentration. The value of $\hat{\mu}$, that is asymptotically Eq. (1) as $t \gg 1$,
 162 gives the future concentration and $\hat{\sigma}$ the future standard deviation. As described in the previous
 163 subsections, Eqs. (12), (14) gives the value of γ and σ , with which we calculate $\hat{\mu}$ and $\hat{\sigma}^2$. In
 164 this way, the present method utilizes fluctuations for the behavior of the future concentration.

165 3.3 Comparison between the analytic solution and the Chernobyl data

166 Now we collect the results from previous sections and thereby make a comparison with the
 167 Chernobyl data. We use Eq. (1) as the mean concentration and $\hat{\sigma}$ as the standard deviation from
 168 the mean concentration. Figure 9 shows the comparison of the raw data of Cs-137 at Point 6.0, 8.0,
 169 11.0, 13.0, 21.0, and 60.1.

170 Many studies have reported that the concentration of particle in the atmosphere follows a
 171 log-normal distribution (e.g. Ashok et al., 1997; Eugene and Chan, 1997; Junya et al., 2002), and
 172 this is consistent with the result of the present study.

173 The thick solid lines indicate the mean concentration (Eq. (1)) and the dotted lines correspond to
174 $\pm \hat{\sigma}$, $\pm 2\hat{\sigma}$, and $\pm 3\hat{\sigma}$. In the log-normal distribution, approximately 68.3% of the data should fall
175 within the range of $\pm \hat{\sigma}$, 95.4% in $\pm 2\hat{\sigma}$, and 99.7% in $\pm 3\hat{\sigma}$. Table 2 gives the percentages for the
176 present study. Our result is consistent with the theoretical percentages.

177 Finally, we mention the significance of our result from a practical aspect. Understanding the
178 distribution of concentration helps us to make estimations of the risk of radiation exposure of
179 workers. Consider the case as follows. In Fukushima, the working hours of workers are determined
180 using the mean atmospheric concentration. In this case, if the concentration is increased temporarily
181 by fluctuations, workers of some percentage might be exposed to excessive radiation. By using the
182 proposed model, we can calculate a possible maximum risk of workers.

183 4. Conclusion

184 We have studied the fluctuations in the atmospheric concentration of Cs-137 in Chernobyl. We
185 found the followings.

- 186 1. We proposed a new method to extract the characteristics of fluctuations. We define the
187 fluctuations as the deviations from Eq. (1). Two parameters, γ (the magnitude of reverse effect)
188 and σ (the magnitude of white noise), represent the characteristics. We showed the procedure of
189 calculating γ and σ from the actual data.
- 190 2. We derived the analytic solution of the long-term concentration with the inclusion of random
191 fluctuations with γ and σ .
- 192 3. The concentration of the Chernobyl data agrees excellently with the solution.
- 193 4. Using these results, we can estimate workers' radiation exposure in Fukushima with uncertainty,
194 with which we know the probability that their exposure falls within the range of $\pm\sigma, \pm 2\sigma, \pm 3\sigma$.

195 Acknowledgment

196 The authors wish to acknowledge NIPPON STEEL CORPORATION, for financial support of this
197 research. The authors would like to thank Dr. Yusuke Uchiyama for comments and discussion on
198 this manuscript and Dr. H. Amano (Toho Univ.) and Dr. T. Ueno (JAEA) for the data.

199 Notation

- A Constant that is proportional to the amount of nuclide that fell in observation point.
- C Radionuclide concentration in the atmosphere.
- C_0 Radionuclide concentration that is observed at time of t .
- $E[]$ Expected value.

- p Transition probability density function of X .
- t The number of days since accident.
- t_0 Measurement date of the first post-accident.
- t_i The i -th measurement day.
- $V[]$ Variance.
- W Wiener process.
- x Random variable representing the value of X at time t .
- x_0 X value at t_0
- X Difference in log axis of the observed value and the average concentration.
- Y Random variable.
- α Constant representing the effect of advection and uptake of plant.
- γ Model parameter indicating earliness of fluctuations converge.
- $\hat{\mu}$ Mean of X .
- λ_{phys} The rate constant which includes all the first-order reactions.
- σ Model parameter indicating the magnitude of the fluctuation.
- $\hat{\sigma}$ Variance of X .

200 Reference

201 Adams, E. E., and L. W. Gelhar (1992), Field study of dispersion in a heterogeneous aquifer, 2,
 202 spatial moment analysis, *Water Resources Research*, 12, 3293-3308. DOI: 10.1029/92WR01757.

203 Arkhipov N. P., N. D. Kuchma, S. Askbrant, P. S. Pasternak, and V. V. Musica (1994), Acute and
 204 long-term effects of irradiation on pine (*Pinus silvestris*) stands post-Chernobyl, *The Science of the*
 205 *Total Environment*, 157, 383-386.

206 Ashok, K. S., S. Anita, E. Engelhardt (1997), The Lognormal Distribution in Environmental
 207 Applications,

208 Eugene, Y., R. Chan (1997), A simple model for the probability density function of concentration
 209 functions in atmospheric plumes, *Atmospheric Environment*, 31, 991-1002.

210 Firestone, R. B., and V. B. Shirley (1996), Table of isotopes, 8E, John Wiley & Sons, New York.

- 211 Hatano, Y., N. Hatano, and A. Suzuki (1995), Dynamic analysis of nuclide diffusion with
212 illitization of the buffer material, *Waste Management*, 16, 495-500.
- 213 Hatano, Y., and N. Hatano (1997), Fractal fluctuation of aerosol concentration near Chernobyl,
214 *Atmospheric Environment*, 31, 2297-2303.
- 215 Hatano, Y., N. Hatano, T. Ueno, H. Amano, A. K. Sukhorchkin, and S. V. Kazakov (1998), Aerosol
216 migration near Chernobyl: long-term data and modeling, *Atmospheric Environment*, 32, 2587-2594.
- 217 Junya, H., K. Nakamura, I. Koichuro, Y. Tokiko, W. Nobuko, M. Hatuhiro, S. Mataka,
218 Characteristics of Concentration Distribution of Hazardous Air Pollutants (HAPs) measured by a
219 Continuous Monitoring System, *Tokyo-to kankyokagaku kenkyuzyo nenpo 2002*, 3-11.
- 220 IAEA(2006), Environmental consequences of the Chernobyl accident and their remediation: twenty
221 years of experience, Report of the Chernobyl Forum Expert Group 'Environment', International
222 Atomic Energy Agency, Vienna, Austria.
- 223 Ishikawa, H. (1995), Evaluation of the Effect of Horizontal Diffusion on the Long-Range
224 Atmospheric Transport Simulation with Chelnobyl Data, *journal of Applied Meteorology*, 34,
225 1653-1665.
- 226 Klug, W., G. Graziani, G. Grippa, D. Pierce, and C. Tassone (1992), Evaluation of Long Range
227 Atmospheric Transport Models using Environmental Radioactivity Data from the Chernobyl
228 Accident, Technische Hochschule Darmstadt, Darmstadt, Germany.
- 229 Lazjukd, G. I, D. L. Nikokaevi, and I. V. Novikova (1997), Changes in Registered Congenital
230 Anomalies in the Republic of Belarus after the Chernobyl Accident, *Stem Cells*, 15, 255-260,
231 doi: 10.1002/stem.5530150734
- 232 Nicholson, K. W. (1998), Review article a review of particle resuspension, *Atmospheric*
233 *Enuinnment*, 22, 2639-2651

- 234 Ould-Dada, Z., and Nasser M. Baghini (2001), Resuspension of small particles from tree surfaces,
235 *Atmospheric Environment*, 35, 3799-3809.
- 236 Romanenko, A. Y., S. C. Finch, M. Hatch, J. H. Lubin, V. G. Bebeshko, D. A. Bazyka, N.
237 Gudzenko, I. S. Dyagil, R. F. Reiss, A. Bouville, V. V. Chumak, N. K. Trotsiuk, N. G. Babkina, Y.
238 Belyayev, I. Masnyk, E. Ron, G. R. Howe, and L. B. Zablotska (2008), The Ukrainian-American
239 Study of Leukemia and Related Disorders among Chernobyl Cleanup Workers from Ukraine: III.
240 Radiation Risks, *Radiation Research*, 170, 691-697, doi: 10.1667/RR1403.1.
- 241 Scargle, J. D. (1982), Studies astronomical time series analysis. II. Statistical aspects of spectral
242 analysis of unevenly spaced data, *The Astrophysical Journal*, 263, 835-853.
- 243 Schulza, M., and K. Stattegger (1997), Spectrum: spectral analysis of unevenly spaced
244 paleoclimatic time series, *Computers & Geosciences*, 23, 929-945.
- 245 Susanne, D., and D. Ove (2008), Parameter estimation from observations of first-passage times of
246 the Ornstein-Uhlenbeck process and the Feller process, *Probabilistic Engineering Mechanics*, 23,
247 170-179.
- 248 Ueno, T., T. Matsunaga, H. Amano, Y. Tkachenko, A. Kovalyov, A. Sukhoruchkin, and V.
249 Derevets (2003), Environmental monitoring data around the Chernobyl nuclear power plant used in
250 the cooperative research project between JAERI and CHESCIR, Japan Atomic Energy Research
251 Institute, Tokai-mura, Naka-gun, Ibaraki-ken.

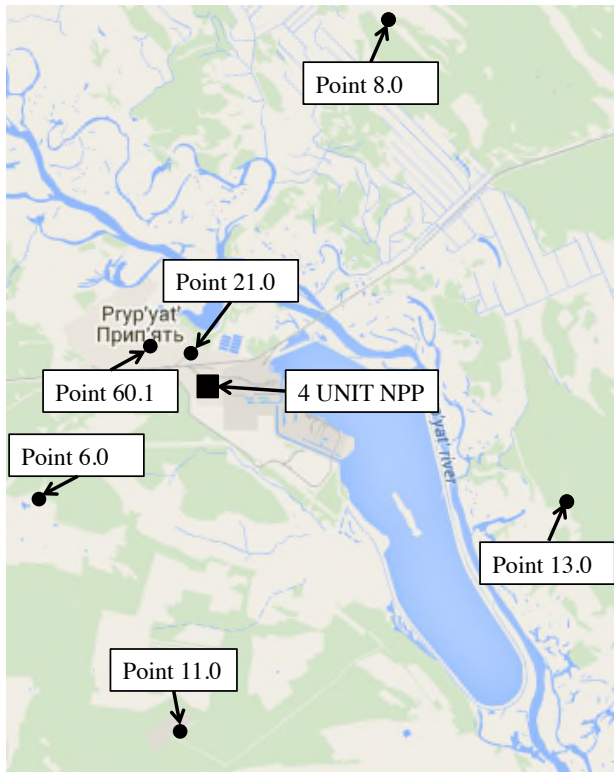


Fig. 1: The location of the Chernobyl power plant and the measurement site. “4 UNIT NPP” indicates the fourth unit of the nuclear power plant, where the accident occurred. Annotations on the Google map.

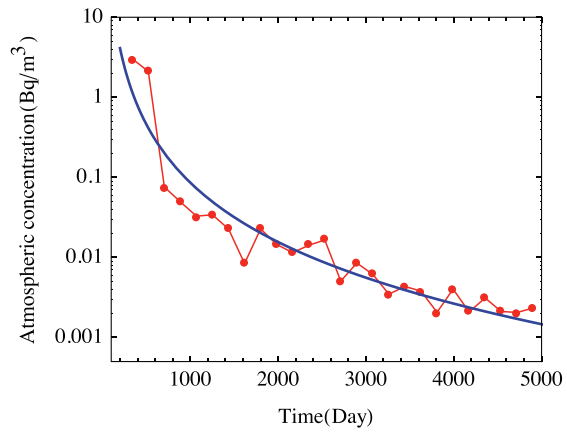


Fig. 2: Atmospheric concentration of 6-months average at Point 21.0.

48
49
50
51
52
53
54
55
56
57
58
59
60
61
62
63
64
65
66
67
68
69
70
71
72
73
74
75
76
77
78
79
80
81
82
83
84
85
86
87
88
89
90
91
92
93
94
95
96
97

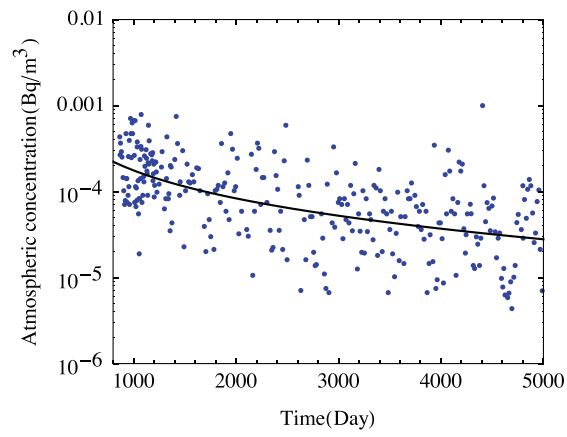


Fig. 3: Atmospheric concentration of Cs-137 at Point 13.0. Dots are the non-averaged original data and the solid line Eq.(1).

98
99
100
101
102
103
104
105
106
107
108
109
110
111
112
113
114
115
116
117
118
119
120
121
122
123
124
125
126
127
128
129
130
131
132
133

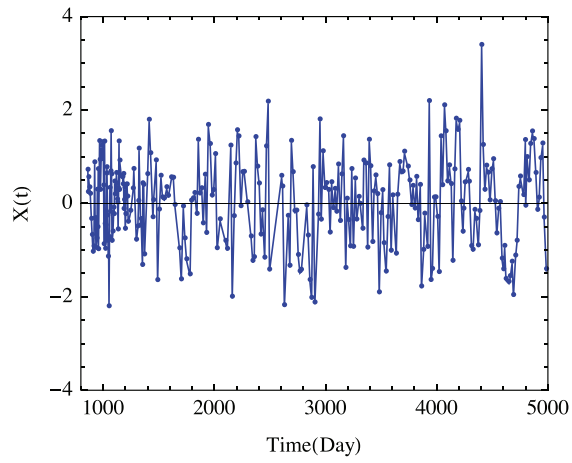


Fig. 4: Deviations $X(t)$ defined as Eq. (2).

134
135
136
137
138
139
140
141
142
143
144
145
146
147
148
149
150
151
152
153
154
155
156
157
158
159
160
161
162
163
164
165
166
167
168

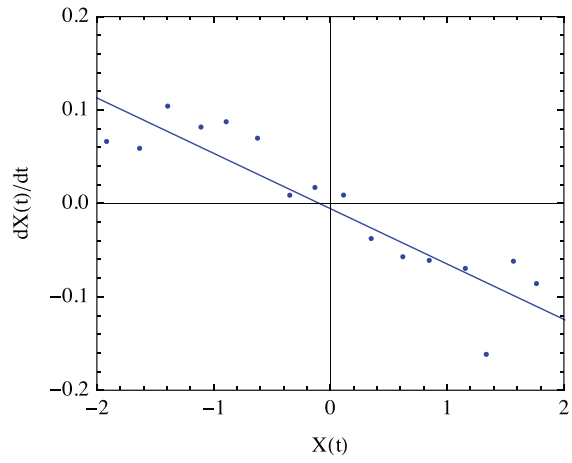


Fig. 5: Relation between $X(t)$ and $dX(t)/dt$.

169
170
171
172
173
174
175
176
177
178
179
180
181
182
183
184
185
186
187
188
189
190
191
192
193
194
195
196
197
198
199
200
201
202

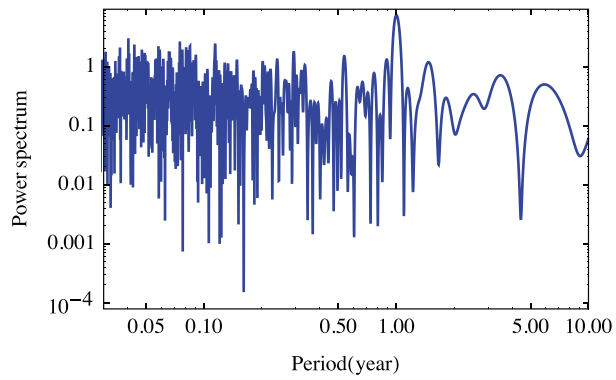


Fig. 6: Power spectrum of the Brownian part $dX + \gamma X dt$. The data of Point 21.0 are used. The spectrum shows the data are white noise.

203
204
205
206
207
208
209
210
211
212
213
214
215
216
217
218
219
220
220
221
222
223
224
225
226
227
228
229
230
231
232
233
234
235
236
237

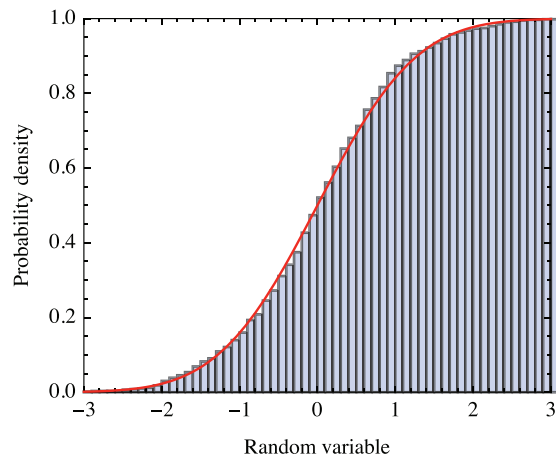
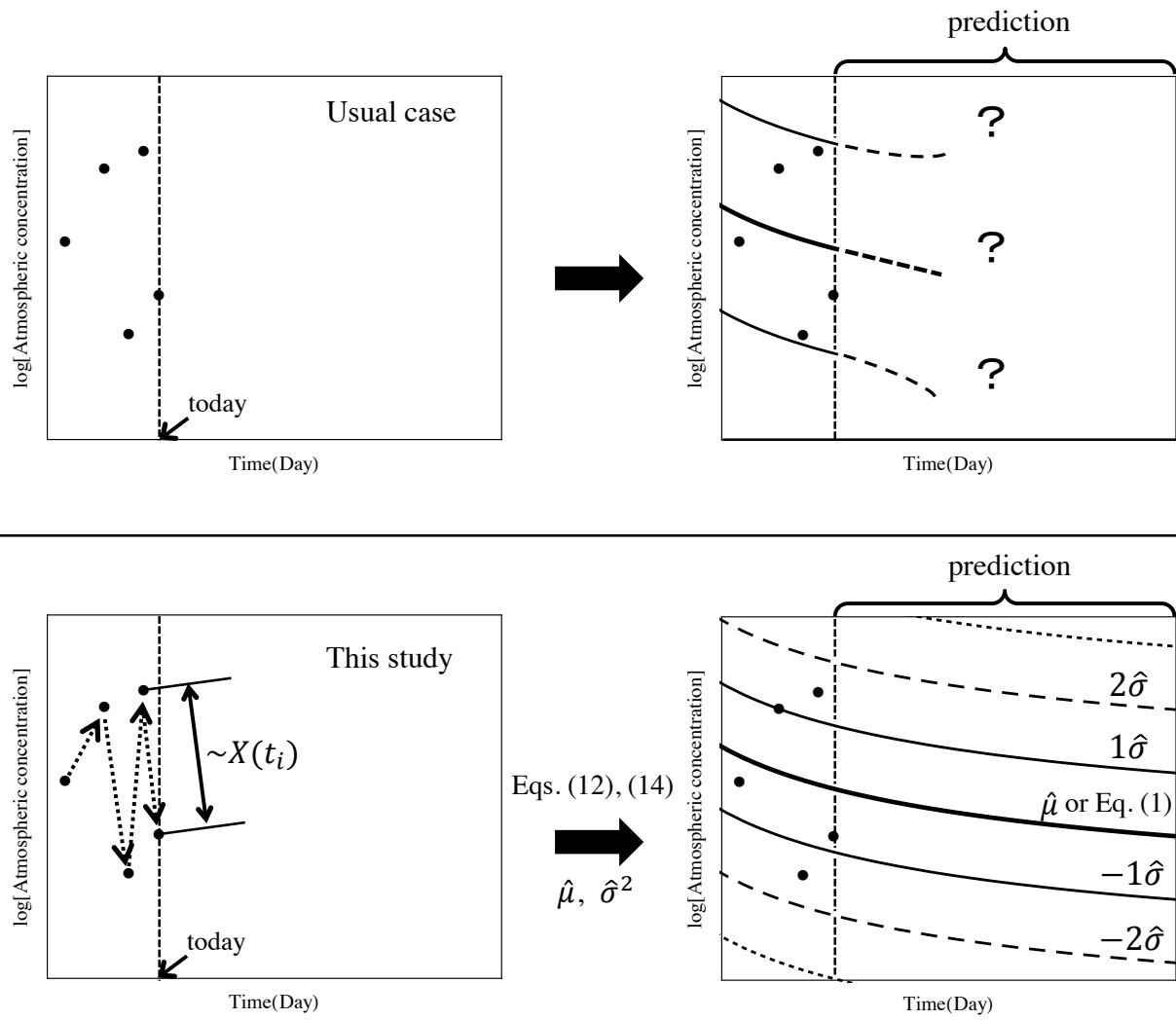


Fig. 7: Histogram of the $dX + \gamma X dt$. It follows the normal distribution. The data is Point 21.0.

238
239
240
241
242
243
244
245
246
247
248
249
250
251
252
253
254
255
256
257
258
259
260
261
262
263
264
265
266



267

Fig. 8: Illustration of the significance of the present model. (upper half): usual case; (lower half): the present study.

268

269

270

271

272

273

274

275

276

277

278

279

280

281

282

283

284

285

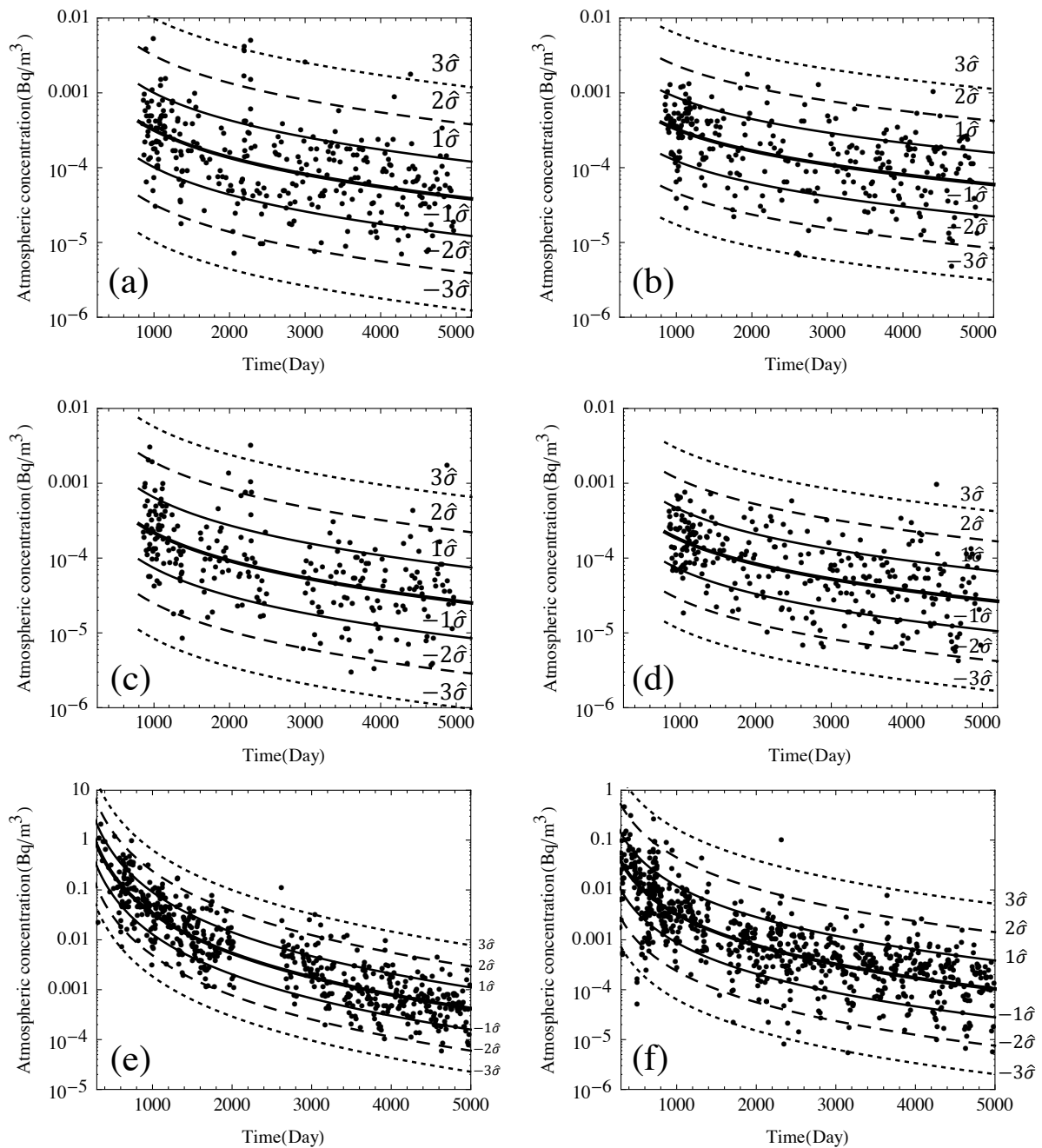


Fig. 9: Standard deviation of fluctuations added to the mean concentration. Curves indicate $\pm\sigma$, $\pm2\sigma$, $\pm3\sigma$. (a) Point 6.0, (b) Point 8.0, (c) Point 13.0, (d) Point 11.0, (e) Point 21.0, (f) Point 60.1. In Point 21.0 and Point 60.1, observation sites are close to the reactor; the atmospheric concentration is higher than other cases, and earlier data are available (since 300 days after the accident). Even such cases, the fluctuations are within the given curves.

286
287

288
289
290
291
292
293

Table 1: The values of γ and σ in each observation site

Site number	A	α	γ	σ
Point 6.0	0.785	1.12	0.393	1.01
Point 8.0	0.118	0.846	0.314	0.779
Point 11.0	0.649	1.15	0.415	0.992
Point 13.0	0.173	0.988	0.371	0.794
Point 21.0 ^a	3.07×10^6	2.63	0.280	0.791
Point 60.1 ^a	2.84×10^3	1.97	0.353	1.04

^a Since the sites of Point 21.0 and Point 60.1 are close to the reactor, values of A is very large compared to other sites.

294
295
296
297
298
299
300
301
302
303
304
305
306
307
308
309
310
311
312
313
314
315
316
317
318
319
320
321
322
323
324
325
326
327
328
329
330
331
332
333
334
335
336

Table, 2: The proportion of data within $\pm \hat{\sigma}$, $\pm 2\hat{\sigma}$, and $\pm 3\hat{\sigma}$.

Code number	$\pm 1\hat{\sigma}$ range	$\pm 2\hat{\sigma}$ range	$\pm 3\hat{\sigma}$ range
Point 6.0	0.724	0.941	0.986
Point 8.0	0.709	0.957	0.996
Point 11.0	0.720	0.947	0.992
Point 13.0	0.671	0.963	0.997
Point 21.0	0.691	0.950	0.997
Point 60.1	0.740	0.933	0.988
Average	0.709	0.949	0.993

338

339

340

341

342

343

344

345

346

347

348

349

350

351

352

353

354

355

356

357

358

359

360

361

362

363

364

365

366

367

368

369

370

371

372

373

374